GEOPHYSICAL RESEARCH LETTERS, VOL. 40, 5932–5936, doi:10.1002/2013GL058267, 2013

Wind-driven mixing causes a reduction in the strength of the continental shelf carbon pump in the Chukchi Sea

Claudine Hauri,[1] Peter Winsor,[1] Laurie W. Juranek,[2] Andrew M. P. McDonnell,[1] Taro Takahashi,[3] and Jeremy T. Mathis[4]

Received 10 October 2013; revised 5 November 2013; accepted 12 November 2013; published 25 November 2013.

[1] The Chukchi Sea is thought to be a globally important sink of atmospheric CO_2 due to the summertime drawdown of surface pCO_2 by phytoplankton and subsequent shelf-to-basin transport of CO_2-enriched subsurface waters into the upper halocline of the Arctic Ocean. Here we show that annually occurring storm-induced mixing events during autumn months disrupt water column stratification and stir up remineralized carbon from subsurface waters to the surface, leading to CO_2 outgassing to the atmosphere. Our analysis provides a new understanding of the dynamics of carbon cycling in the region and suggests that late season wind events are strong and frequent enough to significantly decrease the carbon sink strength of the Chukchi Sea on a scale of relevance to the global carbon cycle. These results highlight the importance of obtaining data with more complete seasonal and spatial coverage in order to accurately constrain regional to basin-scale carbon flux budgets. **Citation:** Hauri, C., P. Winsor, L. W. Juranek, A. M. P. McDonnell, T. Takahashi, and J. T. Mathis (2013), Wind-driven mixing causes a reduction in the strength of the continental shelf carbon pump in the Chukchi Sea, *Geophys. Res. Lett.*, *40*, 5932–5936, doi:10.1002/2013GL058267.

1. Introduction

[2] The Chukchi Sea is viewed as a strong sink for carbon dioxide (CO_2) [*Pipko et al.*, 2002; *Bates*, 2006; *Gao et al.*, 2012; *Mathis and Questel*, 2013]. When the inflow of nutrient-rich Pacific water through the Bering Strait is combined with the sustained solar radiation of sea ice-free periods, the Chukchi Sea (<50 m depths) becomes one of the most productive ecosystems in the world [*Springer and McRoy*, 1993]. High summertime rates of primary production (~ 470 g C m^{-2} y^{-1}) and relatively low pelagic grazing rates drive down the surface partial pressure of CO_2 (pCO_2) to very low levels and support large fluxes of organic carbon to a biomass-rich benthic ecosystem [*Grebmeier et al.*, 2006]. Dilution by melting ice also contributes to the reduction of surface water pCO_2 [*Robbins et al.*, 2013]. The remineralization of organic matter in the subsurface layer results in high subsurface pCO_2 levels across the Chukchi Sea [*Bates et al.*, 2013; *Mathis and Questel*, 2013; *Pipko et al.*, 2002]. The primary fate of this remineralized carbon is thought to be circulation-driven export of subsurface waters into the upper halocline of the Arctic Ocean [*Bates*, 2006; *Anderson et al.*, 2013]. *Bates* [2006] describes this strong CO_2 sink mechanism as a modified version of the continental shelf carbon pump [*Tsunogai et al.*, 1999].

[3] For these reasons, the Chukchi Sea is thought to be the predominant contributor to CO_2 uptake in the Arctic Ocean, the second largest coastal CO_2 sink of the global oceans [*Chen and Borges*, 2009]. However, the carbon budget assessments for the Chukchi Sea are based on extrapolations of spatially and temporally sparse observations (primarily summertime data from the northeastern Chukchi Sea [*Bates*, 2006; *Gao et al.*, 2012; *Mathis and Questel*, 2013]). Given its relevance to the global carbon budget, it is important to fully elucidate the magnitude and variability of sea-air CO_2 fluxes in the Chukchi Sea.

2. The Fate of Remineralized Inorganic Carbon

[4] Taking advantage of newly available continuous underway pCO_2 measurements along North-South transects from the autumn period, we evaluate the hypothesis that the Chukchi Sea is a strong net CO_2 sink. Continuous underway pCO_2 was measured together with salinity and temperature aboard the USCGC *Healy* in 2011 and 2012 with a precision of ±0.5% using a system consisting of a shower-type water-gas equilibrator and infrared CO_2 gas analyzer, which was calibrated every 4 h using five standard gas mixtures spanning between 100 ppm and 700 ppm mole fraction CO_2 certified by the Earth System Research Laboratory of NOAA (see www.ldeo.columbia.edu/pi/CO2 for the operational and engineering details) [*Takahashi et al.*, 2013]. Measured surface seawater pCO_2 (Figures 1a–1e) were variable on both spatial and interannual scales. In 2011, pCO_2 averaged 424 ± 44 µatm (1 STD), 377 ± 60 µatm and 390 ± 37 µatm in September, October, and November respectively. In 2012, average pCO_2 increased from 199 ± 59 µatm in early August (data not shown) to 312 ± 31 µatm and 329 ± 46 µatm, in September and October, respectively.

[5] The maximum pCO_2 in late October 2011 (Figure 1b) to the southwest of Point Hope coincided with a surface O_2/Ar dissolved gas ratio that was only 90% of the saturation ratio (Figure 1f), indicating a strong respiratory signal in surface waters. The October 2011 O_2/Ar observations were determined using an equilibrated inlet mass spectrometer system [*Cassar et al.*, 2009] supplied by the underway

[1]School of Fisheries and Ocean Sciences, University of Alaska Fairbanks, Fairbanks, Alaska, USA.
[2]College of Earth, Ocean, and Atmospheric Sciences, Oregon State University, Corvallis, Oregon, USA.
[3]Lamont-Doherty Earth Observatory, Columbia University, Palisades, New York, USA.
[4]Pacific Marine Environmental Lab, NOAA, Seattle, Washington, USA.

Corresponding author: C. Hauri, School of Fisheries and Ocean Sciences, University of Alaska Fairbanks, Fairbanks, AK 99775-7220, USA. (chauri@alaska.edu)

0094-8276/13/10.1002/2013GL058267

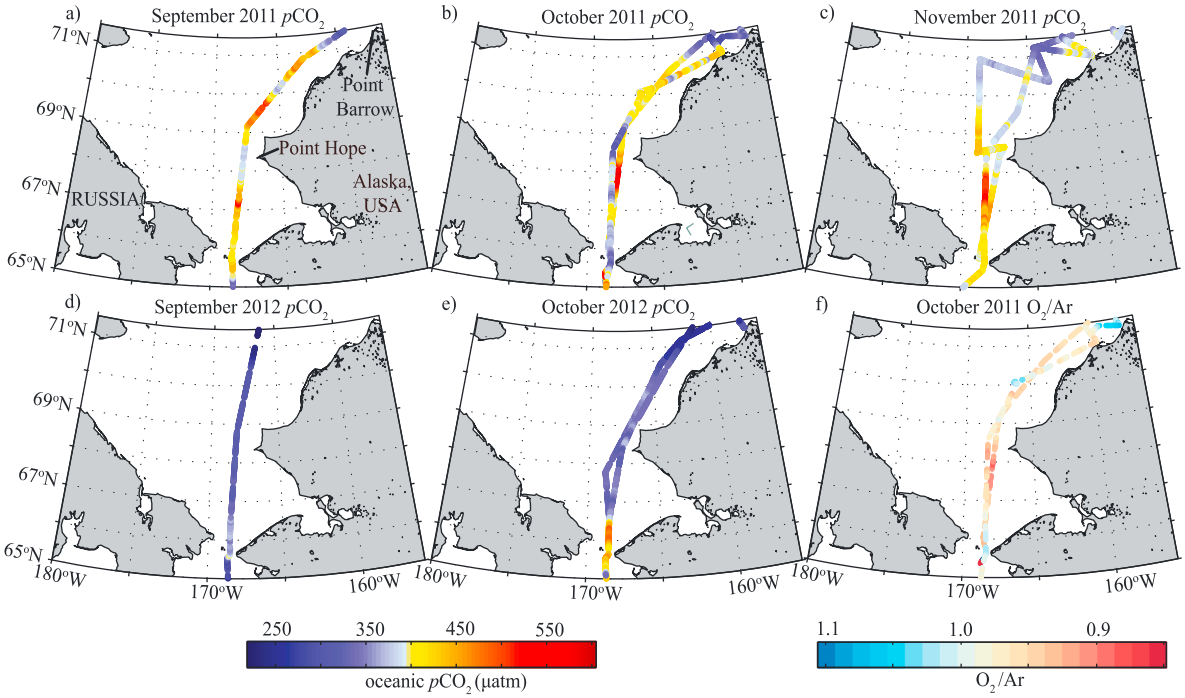

Figure 1. Late season surface pCO_2 and biological O_2 supersaturation in the Chukchi Sea. Shown are surface pCO_2 in (a) September, (b) October, and (c) November 2011, and (d) September, and (e) October 2012. Orange to red colors indicate that surface waters are supersaturated with regard to pCO_2. (f) Biological O_2 supersaturation in October 2011. Values <1 (yellow-red) show that the surface waters were net heterotrophic, while values >1 indicate that the waters were net autotrophic.

seawater line. Surface salinities were also relatively high (>31), which leads us to hypothesize that vertical mixing had recently redistributed subsurface waters throughout the water column. Due to the moderately warm temperatures (2–4°C) and long distance from the shelf break (>500 km), the influence of shelf break upwelling of CO_2-rich deep Arctic Ocean water, as was observed in the Beaufort Sea [*Else et al.*, 2012; *Mathis et al.*, 2012], can be neglected.

[6] To establish a physical basis for the role of vertical mixing in elevating surface pCO_2, we estimated the mixing potential from wind stress on the ocean, using a June–November 2011 time series of 3-hourly estimates of winds near Point Hope (68°N, 168°W, Figure 2b) extracted from the National Center for Environmental Prediction North American Regional Reanalysis (NARR) model hindcasts [*Mesinger et al.*, 2006]. The rate of energy transfer from the wind into the water column ($J\,m^{-2}\,s^{-1}$) is

$$\frac{\partial E}{\partial t} = \rho_a m C_d u^3 \tag{1}$$

[*Denman and Miyake*, 1973]. Here, $\rho_a \sim 1.2\,kg\,m^{-3}$ is the air density, $m \sim 10^{-3}$ is an efficiency factor, $C_d \sim 10^{-3}$ is the drag coefficient, and u is the wind speed at 10 m above sea level. The density contrast between the upper mixed layer (density ρ_1, thickness h_1) and the bottom layer (density ρ_2, thickness h_2) over the depth of the water column, expressed in terms of its potential energy content, PE, is given by

$$PE = \frac{1}{2} g h_1 h_2 (\rho_2 - \rho_1). \tag{2}$$

[7] PE ($J\,m^{-2}$) is the amount of energy required to mix the water column and overcome stratification. Climatological mean vertical temperature and salinity profiles from this area (67–69°N and 170–168°W, extracted from the National Oceanographic Data Center (NODC)) give $h_1 = 7$ m, $h_2 = 30$ m, $\rho_1 = 1024.65\,kg\,m^{-3}$, and $\rho_2 = 1026.10\,kg\,m^{-3}$, such that $PE = 1494\,J\,m^{-2}$. We explored the wind energy (WE) of individual wind events by integrating $\partial E/\partial t$ over the duration of an event. The duration of an event was defined as the time when $\partial E/\partial t > 0.2e^{-3}$. Using a threshold value for PE = $1500\,J\,m^{-2}$ we compared WE of each wind event to PE for the June–November period to investigate whether wind events were strong and long enough to break up the stratification and mix the water column.

[8] Wind events in 2011 were generally stronger and longer between September and November than during the summer months (Figures 2b and 2c). The wind speed ranged from 10 to 15 $m\,s^{-1}$ in September and October and up to 20 $m\,s^{-1}$ in November. Periods with high wind speeds lasted between 9 to 12 days in September and October, whereas in November they lasted less than 5 days. Two wind events, one in September and one in October, reached a WE strong enough (>1500 $J\,m^{-2}$) to overcome the stratification and mix the water column (Figure 2d). The maximum pCO_2 level in September ($pCO_2^{max} = 530$ µatm) and October ($pCO_2^{max} = 605$ µatm), along with salinities >31 and temperatures between 2 and 4°C in both months, were measured toward the end of a 9 day long wind event and within the first half of a 12 day long wind event, respectively (Figures 2a and 2b). At the beginning of November, just a few days after the October wind event ended, wind speeds reached 20 $m\,s^{-1}$. Even though this strong November wind event weakened after just 3 days and was technically not long enough to mix up a fully stratified water column (Figure 2d), it is likely that the water column remained mixed due to the

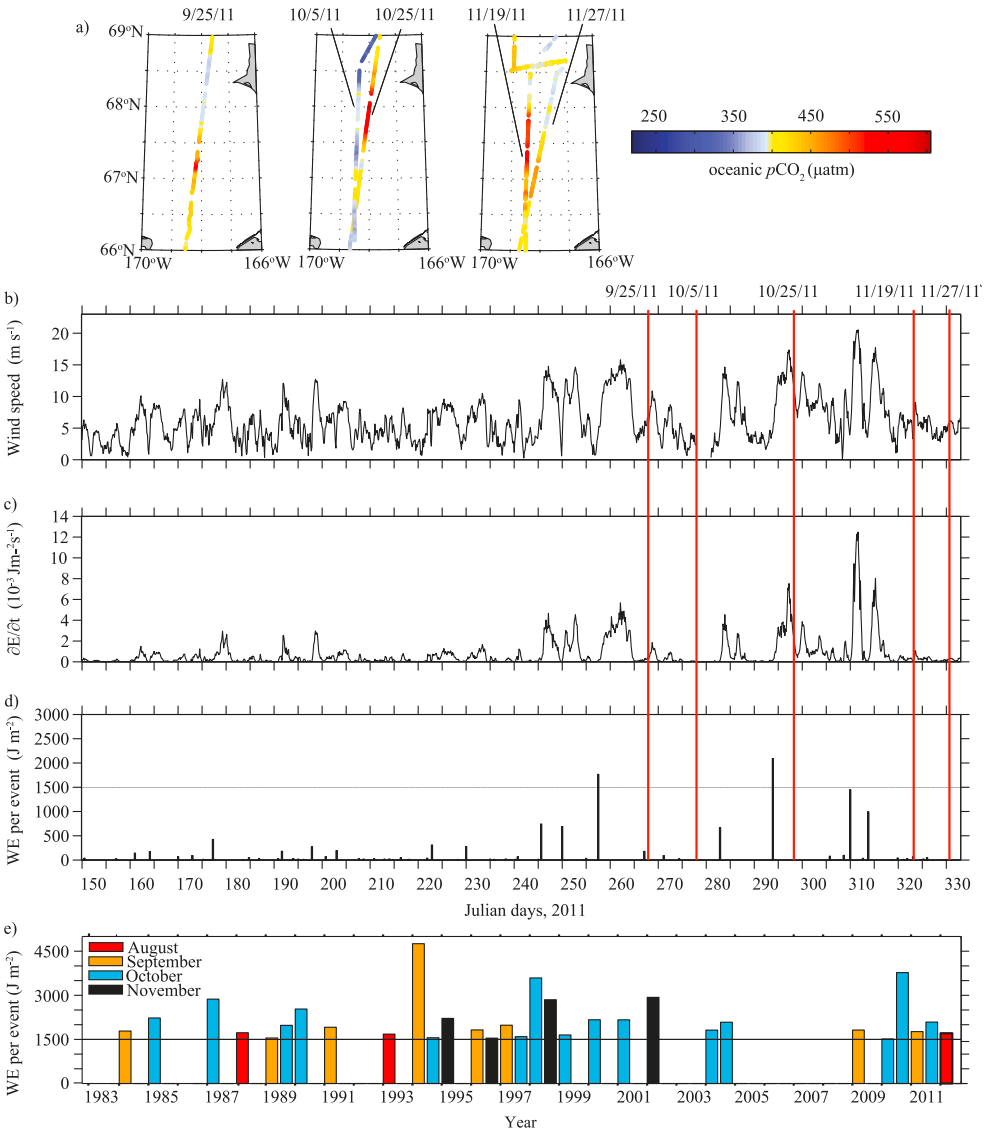

Figure 2. (a) Surface pCO_2 from 2011. Dates indicate day of sampling. Wind products from NARR are (b) wind speed, (c) rate of energy transfer from the wind into the water column ($\partial E/\partial t$), and (d) wind energy (WE) per event for 2011. (e) Events with WE > 1500 J m^{-2} for the NARR time series spanning from 1983 to 2012. Events that were strong and long enough took place in August (red), September (orange), October (blue), and November (black). The horizontal line (PE = 1500 J m^{-2}) indicates the estimated potential energy in the water column due to stratification.

combined effects of heat loss to the atmosphere, sea ice formation, minimal solar gain, and reoccurring strong wind events in November. Measurements of high surface pCO_2 (pCO_2^{max} = 536 µatm; Figure 1), high salinities (>32.5), and low temperatures (<1°C) in middle and end of November 2011 also support this assumption.

[9] Extending the wind analysis beyond 2011 (Figure 2e), we found that winds in late August 2012 were sufficiently strong to mix up the water column. In mid-September, 3 weeks after the wind event, we observed average pCO_2 levels of 312 ± 31 µatm, a significant increase over the levels observed prior to the wind event (199 ± 59 µatm in early August). However, unlike 2011, we did not observe supersaturated pCO_2 levels in surface waters (Figures 1d and 1e). While supersaturation of pCO_2 may have occurred during and immediately following the August event, low surface salinities (25–27) measured in mid-September indicate that freshwater inputs from sea ice melt may have diluted surface pCO_2 below saturation with the atmosphere.

[10] Using monthly averaged NARR winds, we calculated the sea-air CO_2 flux (F) for each surface pCO_2 observation in 2011 and 2012 using

$$F = k\ s\ \Delta pCO_2, \tag{3}$$

where k is the gas transfer velocity (m d^{-1}), and s is the solubility of CO_2 (mmol m^{-3} µatm^{-1}) calculated for observed temperature and salinity [*Weiss*, 1974]. The k was determined using a quadratic wind speed dependency with the proportionality constant 0.31 [*Wanninkhof*, 1992]. The ΔpCO_2 is the difference between oceanic pCO_2 and the monthly mean atmospheric pCO_2 (Point Barrow, Alaska; *Thoning et al.* [2013]; Figure 1a). The spatial averages and standard deviations of the fluxes calculated from these

Table 1. Comparison of Monthly Averaged Sea-Air CO_2 Flux Estimates (mmol C m^{-2} d^{-1})[a]

	2011	2012	*Bates* [2006]
Sep	7.1 ±7.8	−10.1 ±4.4	−40.1
Oct	−1.8 ±8.2	−10.3 ±8.3	−33.0
Nov	−0.9 ±6.0		−15.4

[a]Comparison of autumn sea-air CO_2 fluxes estimated along the ship's tracks of this study with estimates from *Bates* [2006]. The averages and standard deviations of sea-air fluxes from this study were calculated from all fluxes in the area per month. The estimates from *Bates* [2006] were based on linear interpolations of observations taken in 2002 between July/August and May/June sea-air CO_2 fluxes, which were calculated from discrete total alkalinity and dissolved inorganic carbon measurements made in discrete water samples.

observations are presented in Table 1. These flux calculations suggest that the eastern Chukchi Sea was close to equilibrium with the atmosphere in the autumn months of both years, with a weak source potential in September 2011 and a weak sink potential in October and November 2011, and September and October 2012. Localized sea-air fluxes, using shipboard winds compiled by the Shipboard Automated Meteorological And Oceanographic System (SAMOS) data center (http://samos.coaps.fsu.edu), ranged from as low as −64 mmol C m^{-2} d^{-1} in September 2012 to as high as 138 mmol C m^{-2} d^{-1} in October 2011.

3. Wind-Induced Mixing During the Past 30 Years

[11] Late season storm events and resulting mixing are common in the Chukchi Sea. Applying the mixing model described above to the NARR data set over a 30 year period from 1983 to 2012 (for the June–November period) showed that for most years (77%), there was one or two late season wind events with sufficient wind speed and duration to result in an integrated WE input to overcome the assumed stratification (Figure 2e). These wind events occurred most commonly in September and October and were between 4 and 26 days long, with an average wind speed per event ranging between 4 and 15 m s^{-1}. Only two August events and four November events with WE exceeding 1500 J m^{-2} were found over the entire time series. The strongest event of the entire 30 year time series occurred in September 1994 where a large storm system resulted in an integrated WE input of $>$ 4750 J m^{-2}, over 1000 J m^{-2} larger than any other event during the 30 year time series. This storm event had an average wind speed of ~15 m s^{-1}, with peak sustained wind speeds reaching over 18 m s^{-1}.

4. Discussion

[12] These observations offer a revised view of the dynamics of carbon cycling in the Chukchi Sea, where regularly occurring autumn winds mix up CO_2-rich subsurface waters and elevate surface pCO_2 relative to the strongly undersaturated conditions typical of the summer months. By linearly interpolating between observations made in late summer (July/August) and late spring (May/June) in 2002, *Bates* [2006] developed an annual carbon flux estimate for the Chukchi Sea in which 50% of the region's annual uptake of CO_2 occurred during the autumn months when no direct observations were available. This assessment led to sea-air CO_2 flux estimates during the autumn months ranging from −40.1 to −15.4 mmol C m^{-2} d^{-1} (Table 1). In contrast, our direct observations covering complete North-South transects of the Chukchi Sea indicate much weaker uptake or even outgassing of CO_2 to the atmosphere in autumn of two consecutive years. The energetic mixing of the water column in autumn may substantially reduce the overall strength of the Chukchi Sea's continental shelf carbon pump. This process has global implications since the Chukchi Sea is viewed as the predominant driver of CO_2 uptake in the Arctic Ocean, the second largest coastal CO_2 sink globally.

[13] While additional observations and/or numerical modeling would be required to better constrain the annual carbon budget for the Chukchi Sea, there are several reasons to expect that the features and variability we observed may be common across the entire shelf. Strong autumn winds in this region are typically associated with expansive Aleutian low-pressure systems that extend thousands of kilometers toward the Arctic Ocean, resulting in wind patterns that affect the entire Chukchi Sea [*Pickart et al*., 2009]. Furthermore, summertime oceanographic observations show a general pattern of high pCO_2 in subsurface waters across the shelf [*Bates et al*., 2013; *Mathis and Questel*, 2013; *Pipko et al*., 2002]. Together, these conditions indicate that CO_2 is available and likely to be mixed to the surface where it can exchange with the atmosphere.

[14] There are several unaddressed processes that may be responsible for the observed spatial and temporal variability of surface pCO_2 (Figure 1). PE will vary as a result of differences in the water column properties and structure. WE inputs will also vary on local scales. The pCO_2 in subsurface waters is affected by variations in productivity, export, remineralization, and water mass origin. Storm events may also mix up nutrients and potentially trigger a fall phytoplankton bloom [*Else et al*., 2012] and thereby decrease surface pCO_2. Furthermore, horizontal transport of water masses through the region may affect the spatial variability in pCO_2. If the wind events happen as early as August (e.g., 2012), then the potential for restratification is higher because of the influence of residual sea ice melt water, riverine inputs, and solar heating. Stratification is expected to be weaker in late season months than on an annual mean due to heat loss to the atmosphere, sea ice formation in autumn [*Weingartner et al*., 2013], and prior mixing events, and thus our 1500 J m^{-2} estimate of PE is likely a conservative choice (i.e., mixing events may have a lower PE threshold than calculated here, and thus be more frequent). In addition, sea ice formation in November may inhibit the mixing of the water column and the exchange of CO_2 across the sea-air interface.

[15] Climate change is triggering rapid and substantial transformations in the Chukchi Sea and these are likely to impact the cycling of carbon in the region. Increases in storminess [*Walsh et al*., 2012] could enhance CO_2 outgassing in autumn by increasing mixing of the water column. Furthermore, a later onset of sea ice formation will prolong the ocean's exposure to the atmosphere, thereby facilitating additional inputs of wind energy and extending periods of potential outgassing through the ice-free surface. These processes would constitute a positive feedback to climate change by further reducing the carbon sink strength of the Chukchi Sea.

5. Conclusions

[16] Our findings have three major implications. First, they show that the strength of the CO_2 sink in the Chukchi Sea is

substantially lower than previously thought, on a scale of relevance to the global carbon cycle. Second, they call for a reassessment of the importance of the continental shelf carbon pump hypothesis in the Chukchi Sea [*Bates*, 2006], in which shelf-to-basin subsurface transport of carbon is the primary fate of remineralized CO_2. Finally, sparse spatial and seasonal data may not be sufficient to accurately constrain carbon budgets in regions with dynamic physical and biological processes, and we therefore advocate for more comprehensive sampling and mechanistic studies of carbon cycling in these regions.

[17] **Acknowledgments.** We would like to thank the crew of the USCGC *Healy* for their dedicated support of our work. We thank Brent Else and an anonymous reviewer who provided helpful comments on this manuscript. Funding for this work was provided by the National Science Foundation (PLR-1107997 and 1041102-JTM). The pCO_2 system aboard the USCGC *Healy* was engineered by Tim Newberger (U. Colorado) and Scott Hiller (SIO) with support by NOAA grant (NA08OAR4320754) to T.T.

[18] The Editor thanks Brent Else and an anonymous reviewer for their assistance in evaluating this paper.

References

Anderson, L. G., P. S. Andersson, G. Björk, E. P. Jones, S. Jutterström, and I. Wåhlström (2013), Source and formation of the upper halocline of the Arctic Ocean, *J. Geophys. Res. Oceans*, *118*, 410–421, doi:10.1029/2012JC008291.

Bates, N. R. (2006), Air-sea CO_2 fluxes and the continental shelf pump of carbon in the Chukchi Sea adjacent to the Arctic Ocean, *J. Geophys. Res.*, *111*, C10013, doi:10.1029/2005JC003083.

Bates, N. R., M. I. Orchowska, R. Garley, and J. T. Mathis (2013), Summertime calcium carbonate undersaturation in shelf waters of the western Arctic Ocean—How biological processes exacerbate the impact of ocean acidification, *Biogeosciences*, *10*(8), 5281–5309, doi:10.5194/bg-10-5281-2013.

Cassar, N., B. A. Barnett, M. L. Bender, J. Kaiser, R. C. Hamme, and B. Tilbrook (2009), Continuous high-frequency dissolved O_2/Ar measurements by equilibrator inlet mass spectrometry, *Anal. Chem.*, *81*(5), 1855–1864, doi:10.1021/ac802300u.

Chen, C.-T. A., and A. V. Borges (2009), Reconciling opposing views on carbon cycling in the coastal ocean: Continental shelves as sinks and near-shore ecosystems as sources of atmospheric CO_2, *Deep Sea Res., Part II*, *56*(8–10), 578–590, doi:10.1016/j.dsr2.2009.01.001.

Denman, K., and M. Miyake (1973), Behavior of the mean wind, the drag coefficient, and the wave field in the open ocean, *J. Geophys. Res.*, *78*(12), 1917–1931, doi:10.1029/JC078i012p01917.

Else, B. G. T., T. N. Papakyriakou, R. J. Galley, A. Mucci, M. Gosselin, L. A. Miller, and H. Thomas (2012), Annual cycles of pCO_{2sw} in the southeastern Beaufort Sea: New understandings of air-sea CO_2 exchange in arctic polynya regions, *J. Geophys. Res.*, *117*, C00G13, doi:10.1029/2011JC007346.

Gao, Z., L. Chen, H. Sun, B. Chen, and W.-J. Cai (2012), Distributions and air-sea fluxes of carbon dioxide in the Western Arctic Ocean, *Deep Sea Res., Part II*, *81–84*, 46–52, doi:10.1016/j.dsr2.2012.08.021.

Grebmeier, J. M., L. W. Cooper, H. M. Feder, and B. I. Sirenko (2006), Ecosystem dynamics of the Pacific-influenced Northern Bering and Chukchi Seas in the Amerasian Arctic, *Prog. Oceanogr.*, *71*(2–4), 331–361, doi:10.1016/j.pocean.2006.10.001.

Mathis, J. T., and J. M. Questel (2013), Assessing seasonal changes in carbonate parameters across small spatial gradients in the northeastern Chukchi Sea, *Cont. Shelf Res.*, *67*, 42–51, doi:10.1016/j.csr.2013.04.041.

Mathis, J. T., et al. (2012), Storm-induced upwelling of high pCO_2 waters onto the continental shelf of the western Arctic Ocean and implications for carbonate mineral saturation states, *Geophys. Res. Lett.*, *39*, L07606, doi:10.1029/2012GL051574.

Mesinger, F., et al. (2006), North American regional reanalysis, *Bull. Am. Meteorol. Soc.*, *87*(3), 343–360, doi:10.1175/BAMS-87-3-343.

Pickart, R. S., G. W. K. Moore, D. J. Torres, P. S. Fratantoni, R. A. Goldsmith, and J. Yang (2009), Upwelling on the continental slope of the Alaskan Beaufort Sea: Storms, ice, and oceanographic response, *J. Geophys. Res.*, *114*, C00A13, doi:10.1029/2008JC005009.

Pipko, I. I., I. P. Semiletov, P. Y. Tishenko, S. P. Pugach, and J. P. Christensen (2002), Carbonate chemistry dynamics in Bering Strait and the Chukchi Sea, *Prog. Oceanogr.*, *55*, 77–94, doi:10.1016/S0079-6611(02)00071-X.

Robbins, L. L., J. G. Wynn, J. T. Lisle, K. K. Yates, P. O. Knorr, R. H. Byrne, X. Liu, M. C. Patsavas, K. Azetsu-Scott, and T. Takahashi (2013), Baseline monitoring of the Western Arctic Ocean estimates 20% of the Canadian Basin surface waters are undersaturated with respect to aragonite, *PLoS One*, *8*(9), e73796, doi:10.1371/journal.pone.0073796.

Springer, A., and C. McRoy (1993), The paradox of pelagic food webs in the northern Bering Sea—III. Patterns of primary production, *Cont. Shelf Res.*, *13*(5/6), 575–599, doi:10.1016/0278-4343(93)90095-F.

Takahashi, T., S. C. Sutherland, and A. Kozyr (2013), Global ocean surface water partial pressure of CO_2 database: Measurements performed during 1957–2012 (Version 2012), ORNL/CDIAC-160, NDP-088(V2012), Carbon Dioxide Information Analysis Center, Oak Ridge National Laboratory, U.S. Department of Energy, Oak Ridge, Tennessee, doi:10.3334/CDIAC/OTG.NDP088(V2012).

Thoning, K. W., D. R. Kitzis, and A. Crotwell (2013), Atmospheric carbon dioxide dry air mole fractions from quasi-continuous measurements at Barrow, Alaska; Mauna Loa, Hawaii; American Samoa; and South Pole, 1973–2012, Version: 2013-05-28. [Available at ftp://ftp.cmdl.noaa.gov/ccg/co2/in-situ/.]

Tsunogai, S., S. Watanabe, and S. Tetsuro (1999), Is there a "continental shelf pump" for the absorption of atmospheric CO_2?, *Tellus, Ser. B*, *51*(3), 701–712, doi:10.1034/j.1600-0889.1999.t01-2-00010.x.

Walsh, J. E., J. E. Overland, P. Y. Groisman, and B. Rudolf (2012), Ongoing climate change in the Arctic, *Ambio*, *40*(S1), 6–16, doi:10.1007/s13280-011-0211-z.

Wanninkhof, R. (1992), Relationship between wind speed and gas exchange over the ocean, *J. Geophys. Res.*, *97*(C5), 7373–7382, doi:10.1029/92JC00188.

Weingartner, T., E. Dobbins, S. Danielson, P. Winsor, R. Potter, and H. Statscewich (2013), Hydrographic variability over the northeastern Chukchi Sea shelf in summer-fall 2008–2010, *Cont. Shelf Res.*, *67*, 5–22, doi:10.1016/j.csr.2013.03.012.

Weiss, R. (1974), Carbon dioxide in water and seawater: The solubility of a non-ideal gas, *Mar. Chem.*, *2*(3), 203–215, doi:10.1016/0304-4203(74)90015-2.